

## Article

# Spacer Thickness and Temperature Dependences of the Interlayer Exchange Coupling in a Co/Pt/Co Three-Layer Structure

V. S. Gornakov \*, I. V. Shashkov , O. A. Tikhomirov and Yu. P. Kabanov

Osipyan Institute of Solid State Physics RAS, Moscow District, 2 Academician Osipyan Str., Chernogolovka 142432, Russia; shav@issp.ac.ru (I.V.S.); tikhomir@issp.ac.ru (O.A.T.); kabanov@issp.ac.ru (Y.P.K.)

\* Correspondence: gornakov@issp.ac.ru

**Abstract:** Domain wall mobility as a function of nonmagnetic interlayer thickness and temperature was studied in ultrathin exchange-coupled ferromagnetic layers using magneto-optic Kerr microscopy. The system under study is a Pt/Co/Pt/Co/Pt heterostructure having perpendicular magnetic anisotropy and a middle Pt layer with spatially variable thickness. The ferromagnetic interaction between the Co layers is observed when the Pt interlayer thickness varies from 5 to 6 nm in a temperature range of 200–300 K. There is a certain interval of Pt layer thickness where domain walls in both ferromagnetic layers move independently. Nonlinear dependence of the domain wall displacement on the applied field was measured. It is shown that an equilibrium position of the relaxed domain wall depends on field, temperature, and the nonmagnetic interlayer thickness. This position is determined by the energy balance: (i) domain wall displacement provided by the applied field, (ii) interlayer exchange interaction in the area swept by the domain wall, and (iii) domain wall coercivity. The mechanism of domain wall stabilization in terms of independent wall motion near critical thickness was considered. It is found that both the coercivity of the Co layer and the critical thickness decrease at higher temperature, while the interlayer exchange constant  $J$  is changed weakly.

**Keywords:** interlayer exchange coupling; ferromagnetic heterostructure; perpendicular magnetic anisotropy; domain wall; kerr microscopy; temperature



**Citation:** Gornakov, V.S.; Shashkov, I.V.; Tikhomirov, O.A.; Kabanov, Y.P. Spacer Thickness and Temperature Dependences of the Interlayer Exchange Coupling in a Co/Pt/Co Three-Layer Structure.

*Magnetochemistry* **2023**, *9*, 176.  
<https://doi.org/10.3390/magnetochemistry9070176>

Academic Editor: Sujit Das

Received: 29 May 2023

Revised: 3 July 2023

Accepted: 6 July 2023

Published: 8 July 2023



**Copyright:** © 2023 by the authors. Licensee MDPI, Basel, Switzerland. This article is an open access article distributed under the terms and conditions of the Creative Commons Attribution (CC BY) license (<https://creativecommons.org/licenses/by/4.0/>).

## 1. Introduction

Ultrathin magnetic films and heterostructures possessing perpendicular magnetic anisotropy (PMA) are promising objects for both fundamental studies (formation and evolution of specific domain structure [1–5], thermoactivated domain wall creep [6], Spin Transport [7,8], anomalous Hall effect [7,9], spin pumping [8], and spin-wave dynamics [10]) and applications (high-density magnetic memory devices [11,12], magnetic sensors for medicine [13], and superfast elements for spintronics [14]). The intensive study of magnetic heterostructure properties [1–10] is aimed at mechanisms of their magnetization reversal and magnetic transport. The goal is to build adequate theoretical models necessary for the design and optimization of magnetic devices [11–14]. In systems where two ferromagnetic (FM) layers are decoupled by a nonmagnetic (NM) layer, a significant problem is the dependence of magnetization, coercivity, domain wall mobility, and other properties on interlayer exchange interaction  $J = 2 H_J M b$ , where  $H_J$  is the effective field of the interlayer exchange interaction between FM layers, and  $M$  and  $b$  are the magnetization and thickness of FM layers [6]. Further,  $J$  itself depends on both NM interlayer thickness  $t$  and temperature  $T$ . A change in these parameters can critically affect the reliability and working characteristics of magnetic devices.

The magnetization reversal in this material is controlled mainly by the nucleation of opposite domains and by the motion of their domain walls (DWs) [1,5]. These domain transformations are well examined in continuous ultrathin Co films with PMA [15,16].

Similar processes in layered structures are more complicated, where two ferromagnetic (FM) layers are separated by a nonmagnetic (NM) layer [17–21]. Kinetics, relaxation of domain structure, and dynamical parameters of such FM/NM/FM heterophase films are strongly affected by interlayer coupling of exchange  $J$  [1–5,8] or magnetostatic [22] origin. The trilayer objects provide an opportunity for the detailed study of interlayer coupling, manifesting itself in the magnetization reversal of separate layers and of a whole system. The intrinsic feature of exchange coupling is the dependence of interaction on the nonmagnetic layer thickness. It was shown both theoretically [23,24] and experimentally [25,26] that this dependence is oscillatory. The trilayer Co/Au(111)/Co system with a wedge-shaped gold layer was studied in Ref. [26]. By measuring magnetoresistance and the Kerr rotation, the authors show that the mutual orientation of the magnetic moments varies from parallel to antiparallel depending on Au thickness; that is, interaction can be ferromagnetic or antiferromagnetic. Details of the magnetization reversal were not considered. Inhomogeneous nucleation and domain wall motion in trilayers with exchange and magnetostatic interaction were examined in Co/Pt/Co [1–5] and CoPt/NiO/CoPt [22], respectively.

In many such heterostructures [1–6,16,17], the Pt layer thickness utilized in the bottom and top layers would bring Dzyaloshinskii–Moriya interaction (DMI) to the system. The magnetic structures in the FM layer coupled to the Pt layer can arise from interplay with spin stiffness, usual crystallographic anisotropy, and DMI. Due to the Heisenberg-type exchange interaction, the distinct change in magnetization should have a comparatively long scale. As the film is ultrathin, only the in-plane degrees of freedom for such changes exist. Namely, such long-ranged magnetic structures can be found on surfaces around the domain walls of thin magnetic films. Theoretical [27,28] and experimental [1–6,29] papers show that DMI in ultrathin films acts only on its domain structure, while it has no influence on the exchange coupling between two FM layers through the NM spacer when the magnetization of the heterostructures is reversed.

The dependence of the DW velocity on the magnetic field in separate or exchange coupled Co films of different thickness was studied both theoretically and experimentally in [2–5]. The authors observed dynamical coupling of domain walls, which have different mobility in different layers but move together with the same speed in case of ferromagnetic exchange coupling between the layers. In the case of wedge-shaped Co/Pt/Co trilayers [1,5,29], the dependence of  $J$  on the interlayer thickness  $t$  was obtained from minor hysteresis loops or from magneto-optic Kerr visualization of the domain wall motion. It was found that nucleation and motion of domains are uncorrelated in both layers if the interlayer thickness exceeds some critical value  $t_{CR}$ , while the walls move synchronously if the Pt layer is thin. The motion and stabilization of DWs at  $t > t_{CR}$  and value of  $t_{CR}$  itself depend on the properties of both layers, including coercivity and exchange interaction between the layers [29]. Being sensitive to structural defects and coercivity, DW motion should be strongly affected by temperature in addition to interlayer thickness. Currently, this question is not known in detail. In this paper, we study the dynamical properties of domain walls in wedge-shaped Co/Pt/Co trilayers depending on temperature and interlayer thickness.

## 2. Experiment

The Pt(10 nm)/Co(0.6 nm)/Pt( $t$ )/Co(0.6 nm)/Pt(3 nm) structure was synthesized at room temperature using DC magnetron sputtering on the oxidized silicon <111> substrate with dimensions of 50 mm  $\times$  6 mm, with the long direction being the Pt wedge of 10 nm  $\times$  0 nm direction. Sputter deposition was performed at an argon pressure of  $1.5 \times 10^{-3}$  Torr with a base pressure below  $2 \times 10^{-7}$  Torr. Wedge-shaped Pt spacer layers were grown by moving a knife-edge shutter in front of the Co bottom layer during Pt deposition. The sample was cut into 10 pieces and the one with dimensions of 5 mm  $\times$  6 mm was used. Thickness of the Pt layer  $t$  increases uniformly along the sample from 5 to 6 nm. In order to visualize domain structure and measure intensity of a local polar Kerr

effect, we used the polarized microscope POLAM P-312 with the optical cryostat. The hysteresis loops were obtained by measuring the magneto-optic (MO) intensity from local ( $0.3 \times 0.3$ ) mm areas of the sample at the magnetic fields up to  $\pm 500$  Oe. Domain structure and DW motion were registered by the microscope CD camera and analyzed. To improve the magneto-optic contrast, we registered preliminary images of the saturated sample in the strong positive and negative magnetic field. The average of these two magneto-optic pictures was subtracted from every experimental image of transient domain structure. To minimize influence of domain walls from the adjacent layer, the pulse magnetic field was used [29]. The pulse length was chosen so that the wall in the layer with higher coercivity would have no time to follow the fast wall in the first layer.

### 3. Results and Discussion

Before any measurements, the sample was subjected to perpendicular permanent magnetic field  $H = +800$  Oe, and both FM layers were magnetized until saturation. A decrease in this field until zero and its following increase with opposite polarity result in the nucleation of new domains and displacement of their boundaries. At one side of the sample where the nonmagnetic Pt layer is thin, the new domains appear coherently in both FM layers (Figure 1a). The motion of domain walls in this area is also simultaneous (Figure 1b). Local magneto-optic hysteresis loops measured via the Kerr effect are sharply rectangular in this area. It confirms the simultaneous motion of DWs in both layers. This picture is also observed at higher values of Pt thickness  $t$  until it reaches the critical value  $t_{CR} = 5.3$  nm. For higher  $t$  kinetics of the magnetization, reversal is different. The new domains in the two layers arise at different fields (Figure 1c), and the domain walls move almost independently (Figure 1d). This process happens first in one FM layer, and only then the second layer is reversed, too. Despite the thickness of both FM layers being the same, it is possible to determine the reversal order of the magnetization in the top  $M_T$  and bottom  $M_B$  layers from the magneto-optic intensity, taking into account its weakening for the bottom layer (see Ref. [29] for details). The analysis of MO data shows that the nucleation and motion of domain walls starts in the top FM layer where the MO signal at the leading wall is stronger. Coercivity values  $H_{C1}$  and  $H_{C2}$  are obtained from the start field for domain walls in the top and bottom layers, respectively. The difference in coercivity allows one to observe the incoherent nucleation of new domains and separated motion of walls in these layers.

The application of a number of magnetic field pulses ( $\pm 100$  Oe, 4 ms) results in the formation of a complicated domain structure (Figure 2a). The mutual orientation of magnetization in the two layers can form four different combinations distinguished by magneto-optic Kerr intensity: (i) all down, (ii) all up, (iii) top layer down, bottom layer up, (iv) top layer up, bottom layer down. Shaking the walls with an ac magnetic field (10 Hz, amplitude close to coercivity) allows one to first reduce the number of walls (Figure 2b) and then to fix the point  $x_0$  corresponding to the boundary between the areas with ferromagnetic and antiferromagnetic interlayer interaction (Figures 2c and 3a). The registration of the Kerr intensity along the wedge confirms that for all  $x > x_0$ , the primary state of the magnetization orientation in both layers is parallel; that is, the interlayer exchange is ferromagnetic.

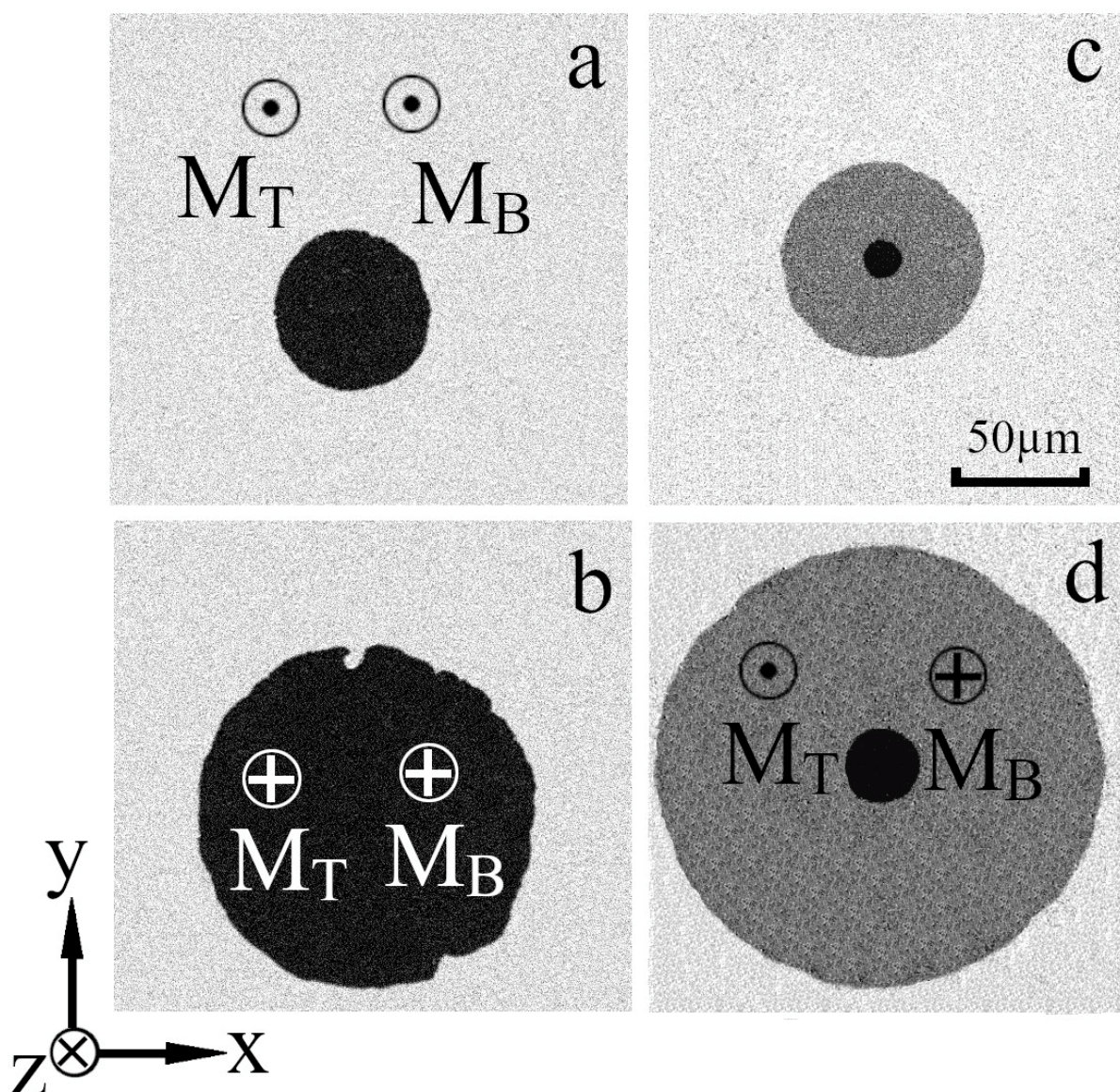


**Figure 1.** Magneto-optic images of nucleation (a,c) and expansion (b,d) of new domains in the FM layers for (a,b)  $t < t_{CR}$  and (c,d)  $t > t_{CR}$ .  $M_T$  and  $M_B$  are magnetization in top and bottom layers, respectively.

Figure 4 shows local hysteresis loops obtained at different temperatures. It can be seen that the coercivity of the sample increases at low temperatures. Steps in the loops at high temperature confirm the difference in coercivity between the upper Co layer and the bottom one. At low temperature, these steps are absent, meaning that the walls in both layers move simultaneously. These loops can be used to obtain the coercivity of both layers at different temperatures; however, more detailed information about the interlayer exchange interaction can be extracted from magneto-optic measurements of the wall motion in the external field, as described in the paper.

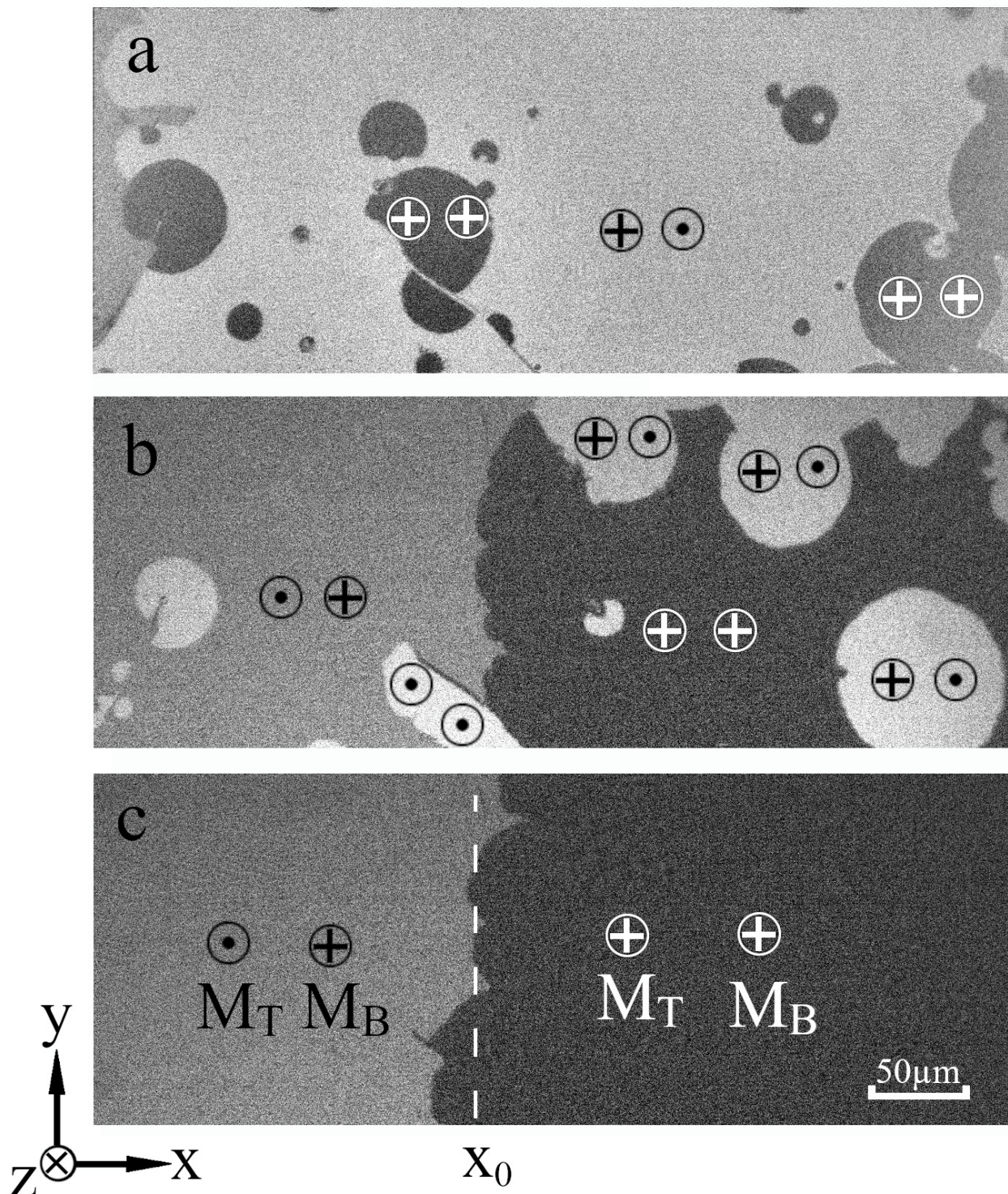


**Figure 2.** Magneto-optic images of (a) domains after application of series of  $\pm 100$  Oe, 4 ms magnetic field pulses, (b) domains after action of ac magnetic field (10 Hz) with amplitude close to coercivity, (c) resulting domain wall between the areas with ferromagnetic and antiferromagnetic interlayer exchange coupling (middle position of the wall  $x_0$  is marked with a dotted line).

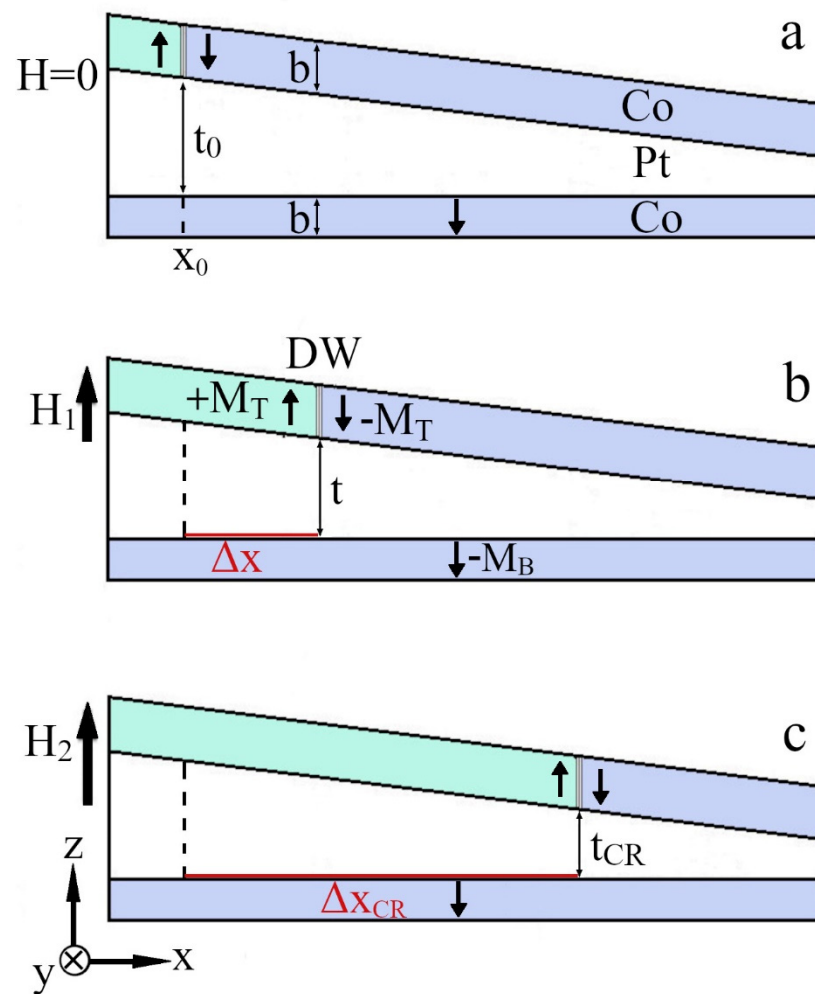


**Figure 3.** Schematic view of the sample (a) in the initial state after formation (Figure 2c) of the boundary between the area with ferromagnetic and antiferromagnetic interlayer interaction, (b) after displacement of the domain wall in the upper FM layer, and (c) after reaching the position with  $t = t_{CR}$ .

The kinetics of the magnetization reversal in the top Co layer at  $t < t_0$  depend drastically on the interlayer thickness, providing that the magnetization  $M_B$  of the bottom layer remains constant. If a series of 4 ms magnetic field pulses is applied to the sample, the distance traveling by the domain wall diminishes from pulse to pulse until the wall stops in some equilibrium position  $x$ , corresponding to a given field amplitude (Figure 3b). For stronger amplitudes, this position tends to be stabilized at  $x = x_{CR}$  (Figure 3c). Figure 4 shows the dependence of the equilibrium position  $x$  on the field amplitude after a series of 5 to 9 pulses with a fixed amplitude. When the field amplitude is larger than the coercivity in the bottom layer  $H_{C2}$ , the second wall starts to move in the bottom layer, so a pulse duration of 4 ms was chosen to separate the motion of these two walls. In this case, the distance between the two walls is much higher than their thickness, and the motion was considered independent. However, the displacement of the two walls equalizes near the critical thickness. Dependence  $x(H)$  is essentially nonlinear tending to saturation at  $x = x_{CR}$ . When the wall in the top layer reaches this point, its independent motion ends, and the wall remains at  $x = x_{CR}$  at all pulse amplitudes until the second wall in the bottom layer joins it. After that, the two walls travel together according to the field amplitude rise. The observed diminishing of the domain wall displacement with every consequent pulse of magnetic field when the wall moves toward the thinner interlayer side (Figure 5) implies

the existence of some effective field  $H_J(x)$ , which is directed against the applied field and whose value rises with the decrease in  $t$ .

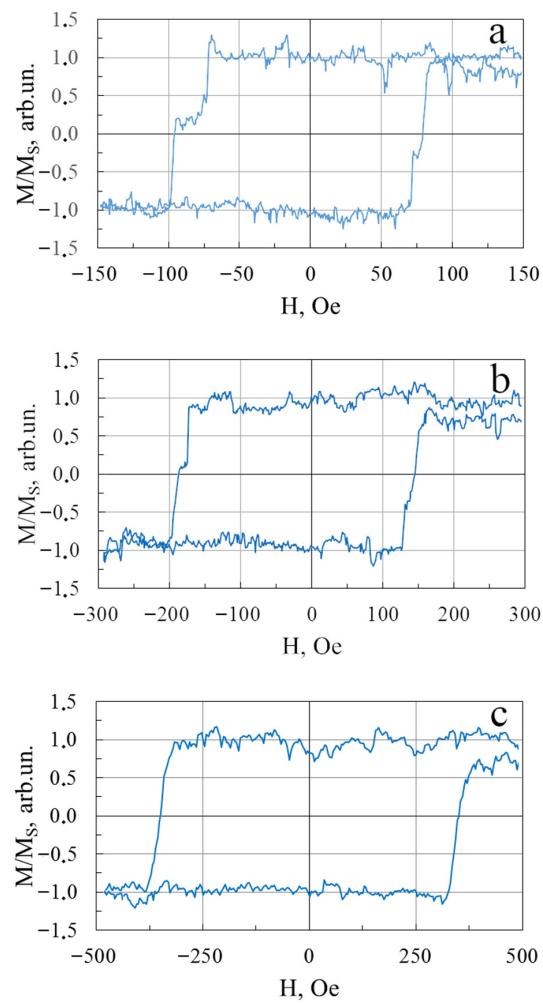


**Figure 4.** Hysteresis loops of the sample at (a)  $T = 293$  K, (b) 250 K and (c) 160 K.

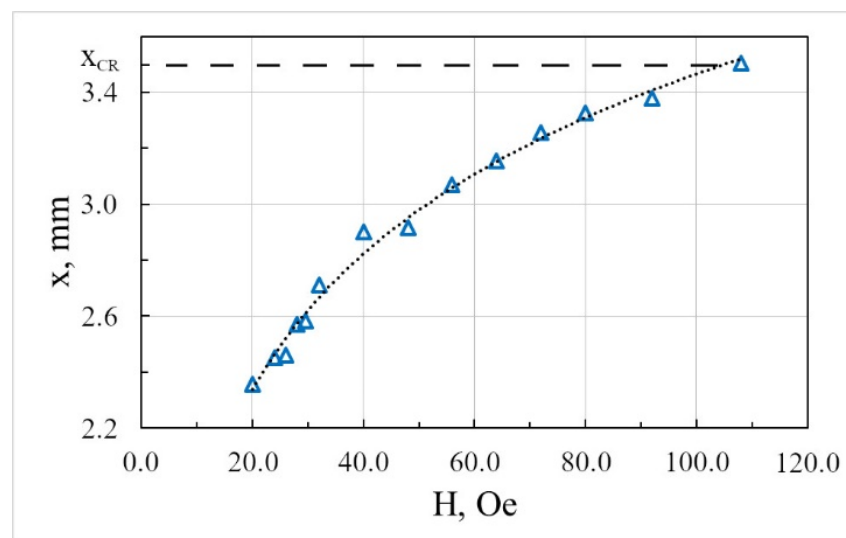


**Figure 5.** Stabilized position of the domain wall as a function of the magnetic field pulse amplitude, room temperature. Dot line is a guide for eyes.

Nonlinear  $x(H)$  dependence has been observed at low temperature, too. Figure 6 shows the DW displacement as a function of the field at different temperatures. It can be seen that the low-temperature motion of the domain walls starts in the region where the nonmagnetic interlayer is thick, and the  $x(H)$  curves shift toward higher fields.

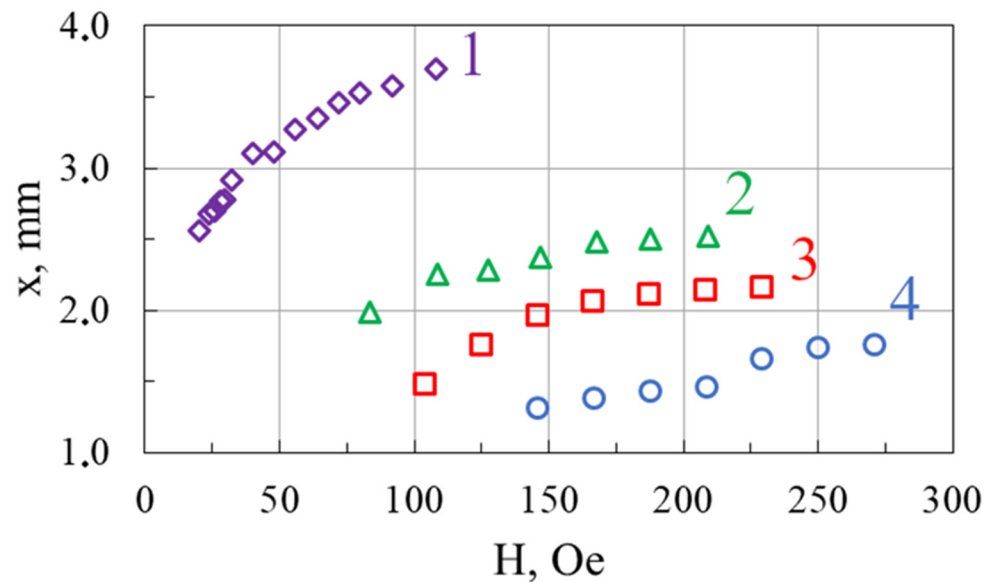


**Figure 6.** Dependence of the stabilized position of the domain wall on the field pulse amplitude at temperatures: 1—293 K, 2—260 K, 3—240 K, 4—220 K.

The change in free energy necessary for the displacement of the wall along the  $x$  axis can be written as

$$\Delta W(x) = 2(H(x) - H_{C1} - H_J(x)) M_T Y b x, \quad (1)$$

where  $b$  is thickness of the FM layer, and  $Y$  is the length of the wall along the  $y$  axis.  $H$  and  $H_{C1}$  are amplitude of the applied field and the coercivity of the top layer, respectively. When the wall stops reaching position  $x$ ,  $\Delta W(x) = 0$ . That means

$$2(H(x) - H_{C1} - H_J(x)) M_T Y b x = 0 \quad (2)$$

or

$$H_J(x) = (H(x) - H_{C1}) \quad (3)$$

The field  $H_J(x)$  is caused by the force exerted by interlayer exchange interaction  $J(t)$  to the wall. As the interlayer thickness decreases linearly along  $x$  with a factor  $C = \Delta t / \Delta x = 1 \text{ nm} / 5 \text{ mm} = 0.2 \text{ nm/mm}$  where  $\Delta t$  is maximal change in the interlayer thickness and  $\Delta x$  is the sample length, the coordinate  $x$  in  $H_J(x)$  can be replaced with  $t$ ,  $t = t_{\text{MAX}} - Cx$ ,  $t_{\text{MAX}} = 6 \text{ nm}$  is maximal interlayer thickness. The obtained nonlinear dependence  $H_J(t)$  is shown in Figure 7. One can see that effective field  $H_J(t)$  grows with the decrease in  $t$ , that is, the increase in  $x$ . The dependence of electric exchange on the distance between atomic layers was discussed recently in [30].

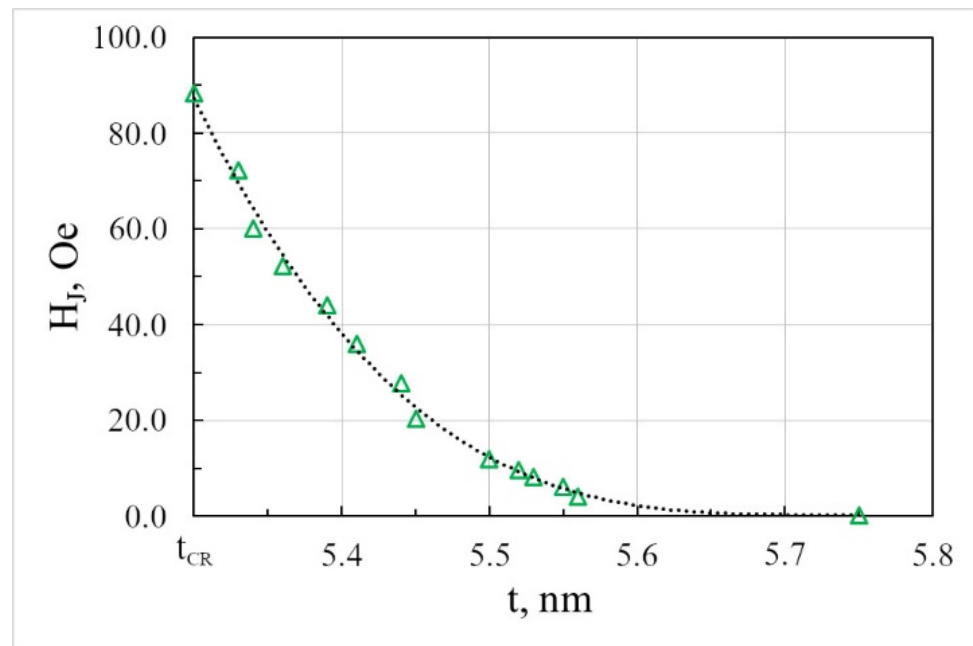


**Figure 7.** Dependence of effective field  $H_J$  on interlayer thickness at room temperature. Dot line is a guide for eyes.

According to (3), the wall moves when  $H(x) - H_J(x) > H_{C1}$ . In the case of  $H(x) - H_J(x) \leq H_{C1}$ , the upper wall should stop, as observed in the experiment. Meanwhile, the bottom wall pursues the first one. The isolated motion besides  $x_{CR}$  is strongly damped. Further enhancement of  $H$  causes joint motion of the two walls, as observed in [1,5]. Nonlinear  $H_J(t)$  dependencies at different temperatures, derived from Figure 6, are shown in Figure 8. Replacing  $x$  with  $t$ , we obtain the detailed dependence  $H_J(t, T)$  for ferromagnetic exchange in the  $H_J(t_{CR}) > H_J(t) > 0$  interval, where  $t_{CR}$  corresponds to the  $x_{CR}$ . One can see that the effective field  $H_J(t)$  becomes larger with the diminishing  $t$  (that is, enhancement of  $x$ ). The results show that the  $H_J$  value remains between 0 Oe and 125 Oe, depending on the wall position  $x$  along the wedge for the temperature interval 200 K to 300 K. Though the  $H_J(t)$  dependence itself varies insignificantly with temperature (namely, weak rise in  $\Delta H_J/\Delta T$  with  $T$ ), the change in the  $H_J$  value for fixed interlayer thickness is strong.

The obtained results show that the observed stabilization of the domain wall in the top layer in position  $x_{CR}$  where interlayer thickness  $t = t_{CR}$  depends on both the effective field  $H_J$  and coercivity  $H_{C1}$ . To establish the influence of temperature on these values and correlations between  $H_{C1}$  and  $t_{CR}$ , we performed measurements on these data from  $x(H, T)$  and  $H_J(t)$ . The minimum values for all graphs in Figure 6 correspond to the start fields of the domain wall, that is, coercivity fields  $H_{C1}$ . The maximal values of  $x(H)$  correspond to the stabilization points  $x_{CR}$ . Taking into account linear dependence  $t(x)$ , one can obtain the critical thickness  $t_{CR}$  at  $x_{CR}$ . Figure 9a shows the dependence  $t_{CR}$  on temperature  $T$ . We see that critical thickness decreases with  $T$  approximately linearly. Figure 9b shows dependence  $H_{C1}(T)$  determined from measured curves  $x(H)_T$  in Figure 6. This dependence correlates, in general, with  $t_{CR}(T)$ ; however, the change in coercivity is nonlinear.

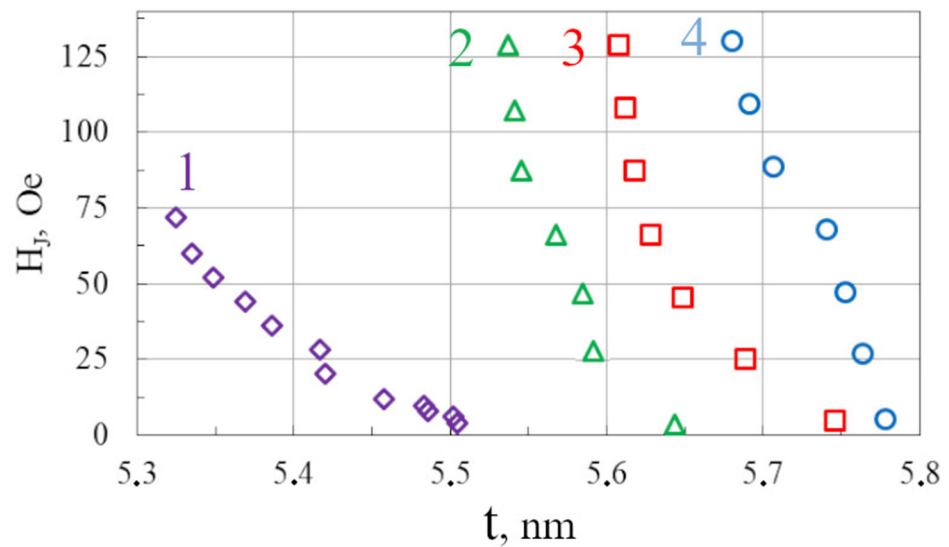


**Figure 8.** Dependence of effective field  $H_J$  on interlayer thickness at temperatures: 1—293 K, 2—260 K, 3—240 K, 4—220 K.

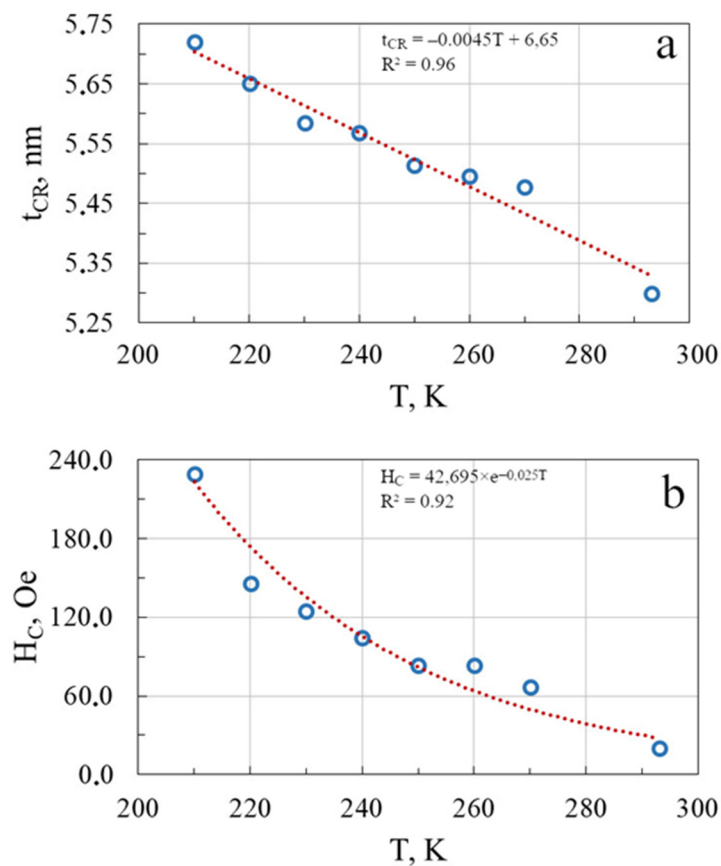


**Figure 9.** Dependencies of (a) critical interlayer thickness and (b) coercive field in the top FM layer on temperature. Dot line is a guide for eyes.

Interlayer exchange between the ferromagnetic layers through the nonmagnetic layer depends on the interlayer properties. It has the same origin as the RKKY interaction between magnetic impurities in the nonmagnetic medium [24]. This interaction due to spin-polarized conductive electrons controls the magnetic properties of such multilayers.

The RKKY theory predicts [24] that for spacer-layer thicknesses,  $t$ , the coupling should be given by a sum of terms in the form

$$J(t) = \sum (J^\alpha / t^2) \sin(q^\alpha t + \varphi^a), \quad (4)$$

where sum is over all critical points, labeled by  $\alpha$ , with critical spanning vector  $q^\alpha$ , coupling strength,  $J^\alpha$ , and phase  $\varphi^a$ . This results in oscillatory behavior of the  $J(t)$  dependence taking both positive and negative values, that is, parallel or antiparallel spin orientation in the ferromagnetic layers. The oscillation period is known well, while the  $J(t)$  dependence itself is not studied in detail in the case of ferromagnetic interaction between the layers. Our work presents such information determined experimentally via direct measurement of the effective exchange field with its compensation by the external magnetic field, as described above.

Further, the RKKY models predict a specific form of the temperature dependence [23], including an additional factor in the form

$$(2\pi k_B T t / \hbar v^\alpha) / \sinh(2\pi k_B T t / \hbar v^\alpha) \quad (5)$$

associated with each critical spanning vector. One can see that temperature appears here as a product of interlayer thickness. We studied the dependence of the effective field on thickness,  $\Delta H_J / \Delta t$ , at different temperatures (Figure 8). This dependence does not change much at different temperatures, as observed in our experiments.

#### 4. Conclusions

We studied the in-field evolution of domain structure in a magnetic trilayer Co/Pt/Co using magneto-optic Kerr microscopy. To find the dependence of the exchange interaction between the Co layers on Pt thickness and temperature, we measured the displacement of the domain wall as a function of the applied magnetic field. This allowed us to determine the exact value of the effective field  $H_J$  along the wedge-shaped nonmagnetic interlayer. For the first time in an FM/NM/FM trilayer, the dependence of this value on NM thickness has been measured in a temperature range from 200 to 300 K. The formation of the previously discovered [1,5,29] boundary separating the areas with different patterns of the magnetization reversal was studied experimentally at different temperatures. The nonlinear increase in  $H_J(t)$  toward the thinner Pt layer side requires a stronger field to induce the motion of the domain wall in this direction. Separate motion of a domain wall becomes damped, and in a still-stronger field, it is accompanied by the motion of the wall in the second FM layer, as observed in [1,5,29]. Stabilization of the wall at critical thickness of Pt depends on the effective exchange field  $H_J$  and coercivity  $H_{C1}$ . Measured dependencies of  $H_{C1}$  и  $t_{CR}$  on temperature are found to be correlated. As the results obtained using the wedge interlayer samples can be influenced by this shape, we will study the temperature-dependent domain wall mobility in the samples with fixed  $t$  in our following publications. The measured  $J(T)$  dependencies should help to deduce the adequate theory of interlayer exchange interaction in such trilayers.

The paper was conducted in the frame of the state task of ISSP RAS.

**Author Contributions:** Conceptualization, V.S.G.; methodology, Y.P.K. and V.S.G.; formal analysis, V.S.G.; investigation, I.V.S. and Y.P.K.; data curation, I.V.S. and Y.P.K.; writing—original draft preparation, V.S.G. and O.A.T.; writing—review and editing, V.S.G. and O.A.T.; visualization, O.A.T.; supervision, V.S.G.; project administration, V.S.G. All authors have read and agreed to the published version of the manuscript.

**Funding:** This research was performed in the framework of the State Task program of the Institute of Solid State Physics, Russian Academy of Science.

**Institutional Review Board Statement:** Not applicable.

**Informed Consent Statement:** Our study is not involving humans or animals.

**Data Availability Statement:** The data are available from the authors on reasonable demand.

**Conflicts of Interest:** The authors declare no conflict of interest.

## References

1. Shull, R.D.; Iunin, Y.L.; Kabanov, Y.P.; Nikitenko, V.I.; Skryabina, O.V.; Chien, C.L. Influence of Pt spacer thickness on the domain nucleation in ultrathin Co/Pt/Co trilayers. *J. Appl. Phys.* **2013**, *113*, 17C101. [\[CrossRef\]](#)
2. Metaxas, P.J.; Stamps, R.L.; Jamet, J.P.; Ferré, J.; Baltz, V.; Rodmacq, B.; Politi, P. Dynamic binding of driven interfaces in coupled ultrathin ferromagnetic layers. *Phys. Rev. Lett.* **2010**, *104*, 237206. [\[CrossRef\]](#) [\[PubMed\]](#)
3. Politi, P.; Metaxas, P.J.; Jamet, J.P.; Stamps, R.L.; Ferré, J. Model of bound interface dynamics for coupled magnetic domain walls. *Phys. Rev. B* **2011**, *84*, 054431. [\[CrossRef\]](#)
4. Metaxas, P.J.; Stamps, R.L.; Jamet, J.P.; Ferré, J.; Baltz, V.; Rodmacq, B. Expansion and relaxation of magnetic mirror domains in a Pt/Co/Pt/Co/Pt multilayer with antiferromagnetic interlayer coupling. *J. Phys. Condens. Matter* **2012**, *24*, 024212. [\[CrossRef\]](#) [\[PubMed\]](#)
5. Matczak, M.; Schäfer, R.; Urbaniak, M.; Kuświk, P.; Szymański, B.; Schmidt, M.; Aleksiejew, J.; Stobiecki, F. Influence of domain structure induced coupling on magnetization reversal of Co/Pt/Co film with perpendicular anisotropy. *J. Magn. Magn. Mat.* **2017**, *422*, 465–469. [\[CrossRef\]](#)
6. Metaxas, P.J.; Jamet, J.P.; Ferré, J.; Rodmacq, B.; Dieny, B.; Stamps, R.L. Magnetic domain wall creep in the presence of an effective interlayer coupling field. *J. Magn. Magn. Mat.* **2008**, *320*, 2571–2575. [\[CrossRef\]](#)
7. Zhang, F.; Liu, Z.; Wen, F.; Liu, Q.; Li, X.; Ming, X. Magnetoresistance and anomalous Hall effect with Pt spacer thickness in the spin-valve Co/Pt/[Co/Pt] 2 multilayers. *J. Supercond. Nov. Magn.* **2017**, *30*, 533–538. [\[CrossRef\]](#)
8. Omelchenko, P.; Montoya, E.; Girt, E.; Heinrich, B. Interlayer Exchange Coupling, Spin Pumping and Spin Transport in Metallic Magnetic Single and Bilayer Structures. *J. Exp. Theor. Phys.* **2020**, *131*, 113–129. [\[CrossRef\]](#)
9. Liu, Q.; Jiang, S.; Teng, J. Interfacial chemical structure-modulated anomalous Hall effect in perpendicular Co/Pt multilayers. *Appl. Surf. Sci.* **2018**, *433*, 556–559. [\[CrossRef\]](#)
10. Szulc, K.; Mendisch, S.; Mruczkiewicz, M.; Casoli, F.; Becherer, M.; Gubbiotti, G. Nonreciprocal spin-wave dynamics in Pt/Co/W/Co/Pt multilayers. *Phys. Rev. B* **2021**, *103*, 134404. [\[CrossRef\]](#)
11. Moritz, J.; Rodmacq, B.; Auffret, S.; Dieny, B. Extraordinary Hall effect in thin magnetic films and its potential for sensors, memories and magnetic logic applications. *J. Phys. D Appl. Phys.* **2008**, *41*, 135001. [\[CrossRef\]](#)
12. Dieny, B.; Chshiev, M. Perpendicular magnetic anisotropy at transition metal/oxide interfaces and applications. *Rev. Mod. Phys.* **2017**, *89*, 025008. [\[CrossRef\]](#)
13. Katagiri, M.; Cuya Huaman, J.L.; Matsumoto, T.; Suzuki, K.; Miyamura, H.; Balachandran, J. Magneto-plasmonic Co@Pt@Au nanocrystals for biosensing and therapeutics. *ACS Appl. Nano Mater.* **2020**, *3*, 418–427. [\[CrossRef\]](#)
14. Wilson, R.B.; Yang, Y.; Gorchon, J.; Lambert, C.H.; Salahuddin, S.; Bokor, J. Electric current induced ultrafast demagnetization. *Phys. Rev. B* **2017**, *96*, 045105. [\[CrossRef\]](#)
15. Krusin-Elbaum, L.; Shibauchi, T.; Argyle, B.; Gignac, L.; Weller, D. Stable ultrahigh-density magneto-optical recordings using introduced linear defects. *Nature* **2001**, *410*, 444. [\[CrossRef\]](#) [\[PubMed\]](#)
16. Morgunov, R.B.; Yurov, A.V.; Yurov, V.A.; Talantsev, A.D.; Bezverhni, A.I.; Koplak, O.V. Oscillatory dynamics of the magnetic moment of a Pt/Co/Ir/Co/Pt synthetic antiferromagnet. *Phys. Rev. B* **2019**, *100*, 144407. [\[CrossRef\]](#)
17. Morgunov, R.B.; Bezverkhni, A.I.; Hehn, M.; Bello, J.L.; Fache, T.; Mangin, S. Dzyaloshinskii-Moriya interaction probed by magnetization reversal in bilayer Pt/Co/Ir/Co/Pt synthetic ferrimagnets. *Phys. Rev. B* **2021**, *104*, 134424. [\[CrossRef\]](#)
18. Mazalski, P.; Anastaziak, B.; Kuświk, P.; Kurant, Z.; Svekle, I.; Maziewski, A. Demagnetization of an ultrathin Co/NiO bilayer with creation of submicrometer domains controlled by temperature-induced changes of magnetic anisotropy. *J. Magn. Magn. Mat.* **2020**, *508*, 166871. [\[CrossRef\]](#)
19. Hellwig, O.; Berger, A.; Fullerton, E.E. Magnetic reversal and domain structure in perpendicular AF-coupled films. *J. Magn. Magn. Mat.* **2005**, *290–291*, 1–7. [\[CrossRef\]](#)
20. Hellwig, O.; Berger, A.; Kortright, J.B.; Fullerton, E.E. Domain structure and magnetization reversal of antiferromagnetically coupled perpendicular anisotropy films. *J. Magn. Magn. Mat.* **2007**, *319*, 13–55. [\[CrossRef\]](#)
21. Kiselev, N.S.; Bran, C.; Wolff, U.; Schultz, L.; Bogdanov, A.N.; Hellwig, O.; Neu, V.; Rößler, U.K. Metamagnetic domains in antiferromagnetically coupled multilayers with perpendicular anisotropy. *Phys. Rev. B* **2010**, *81*, 054409. [\[CrossRef\]](#)
22. Baruth, A.; Yuan, L.; Burton, J.D.; Janicka, K.; Tsybal, E.Y.; Liou, S.; Adenwalla, S. Domain overlap in antiferromagnetically coupled [Co/Pt]/NiO/[Co/Pt] multilayers. *Appl. Phys. Lett.* **2006**, *89*, 202505. [\[CrossRef\]](#)
23. Bruno, P.; Chappert, C. Ruderman-Kittel theory of oscillatory interlayer exchange coupling. *Phys. Rev. B* **1992**, *46*, 261. [\[CrossRef\]](#)
24. Stiles, M.D. Exchange coupling in magnetic heterostructures. *Phys. Rev. B* **1993**, *48*, 7238. [\[CrossRef\]](#)
25. Parkin, S.S. Systematic variation of the strength and oscillation period of indirect magnetic exchange coupling through the 3d, 4d, and 5d transition metals. *Phys. Rev. Lett.* **1991**, *67*, 3598. [\[CrossRef\]](#)
26. Grolier, V.; Renard, D.; Bartenlian, B.; Beauvillain, P.; Chappert, C.; Dupas, C.; Ferré, J.; Galtier, M.; Kolb, E.; Mulloy, M.; et al. Unambiguous evidence of oscillatory magnetic coupling between Co layers in ultrahigh vacuum grown Co/Au(111)/Co trilayers. *Phys. Rev. Lett.* **1993**, *71*, 3023. [\[CrossRef\]](#)

27. Heide, M.; Bihlmayer, G.; Mavropoulos, P.; Bringer, A.; Blügel, S. Spin orbit driven physics at surfaces. *Newsl. Psi-K Netw.* **2006**, *78*, 111–145.
28. Thiaville, A.; Rohart, S.; Jué, É.; Cros, V.; Fert, A. Dynamics of Dzyaloshinskii domain walls in ultrathin magnetic films. *Europhys. Lett.* **2012**, *100*, 57002. [[CrossRef](#)]
29. Shashkov, I.V.; Kabanov, Y.P.; Tikhomirov, O.A.; Gornakov, V.S. Kinetics of Domain Structure in Co/Pt/Co Ultrathin Films with Ferromagnetic Interlayer Exchange Interaction: Dependence on Interlayer Thickness. *Magnetism* **2022**, *2*, 186–194. [[CrossRef](#)]
30. Kong, S.S.; Liu, W.K.; Yu, X.X.; Li, Y.L.; Yang, L.Z.; Ma, Y.; Fang, X.Y. Interlayer interaction mechanism and its regulation on optical properties of bilayer SiCNSs. *Front. Phys.* **2023**, *18*, 43302. [[CrossRef](#)]

**Disclaimer/Publisher's Note:** The statements, opinions and data contained in all publications are solely those of the individual author(s) and contributor(s) and not of MDPI and/or the editor(s). MDPI and/or the editor(s) disclaim responsibility for any injury to people or property resulting from any ideas, methods, instructions or products referred to in the content.